

Figure 5.1 Schematic diagram of the canal having side slopes lined with loose riprap and bottom unlined

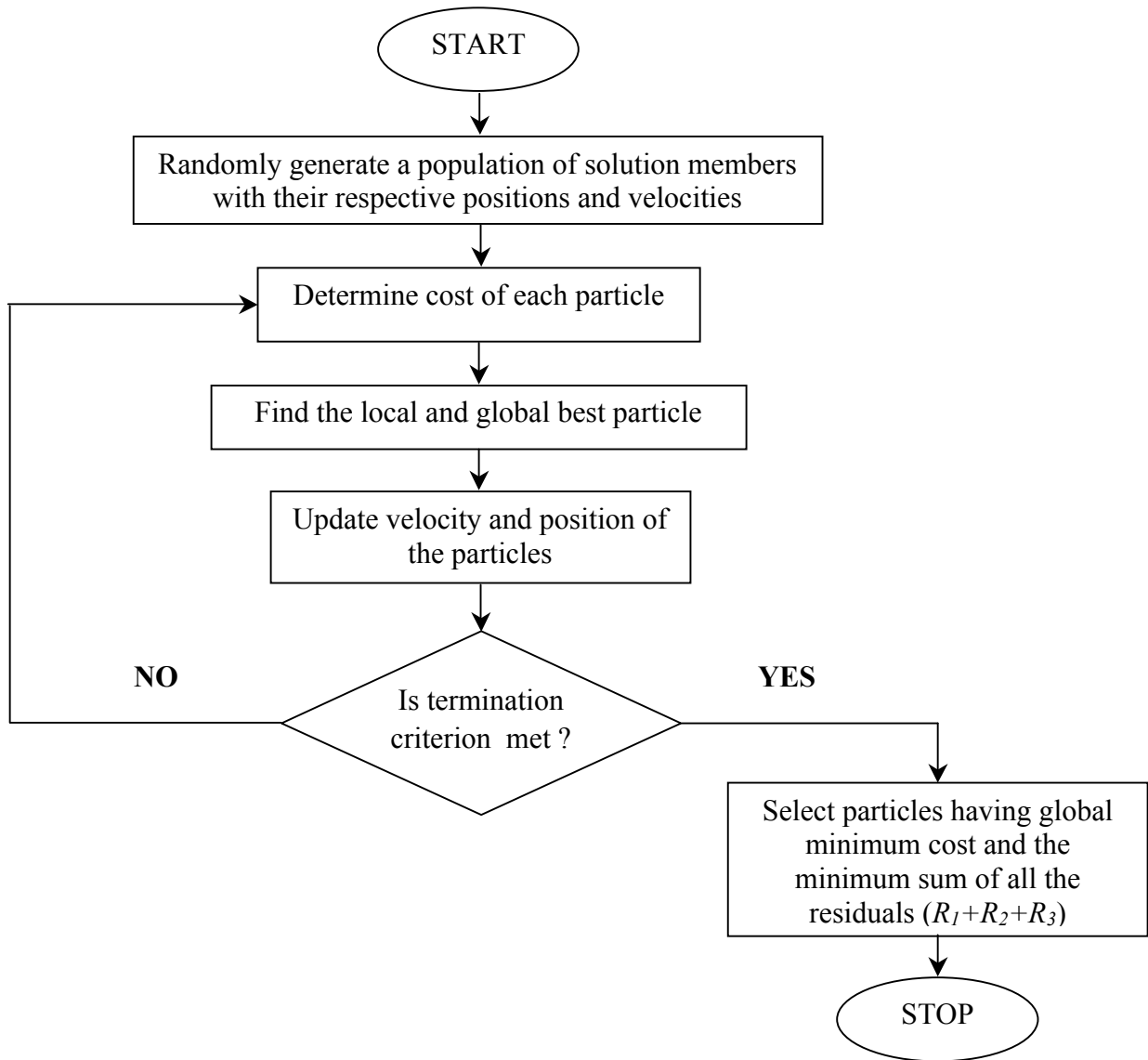


Figure 5.2 Flow chart depicting Particle Swarm Optimization algorithm as applied to the problem

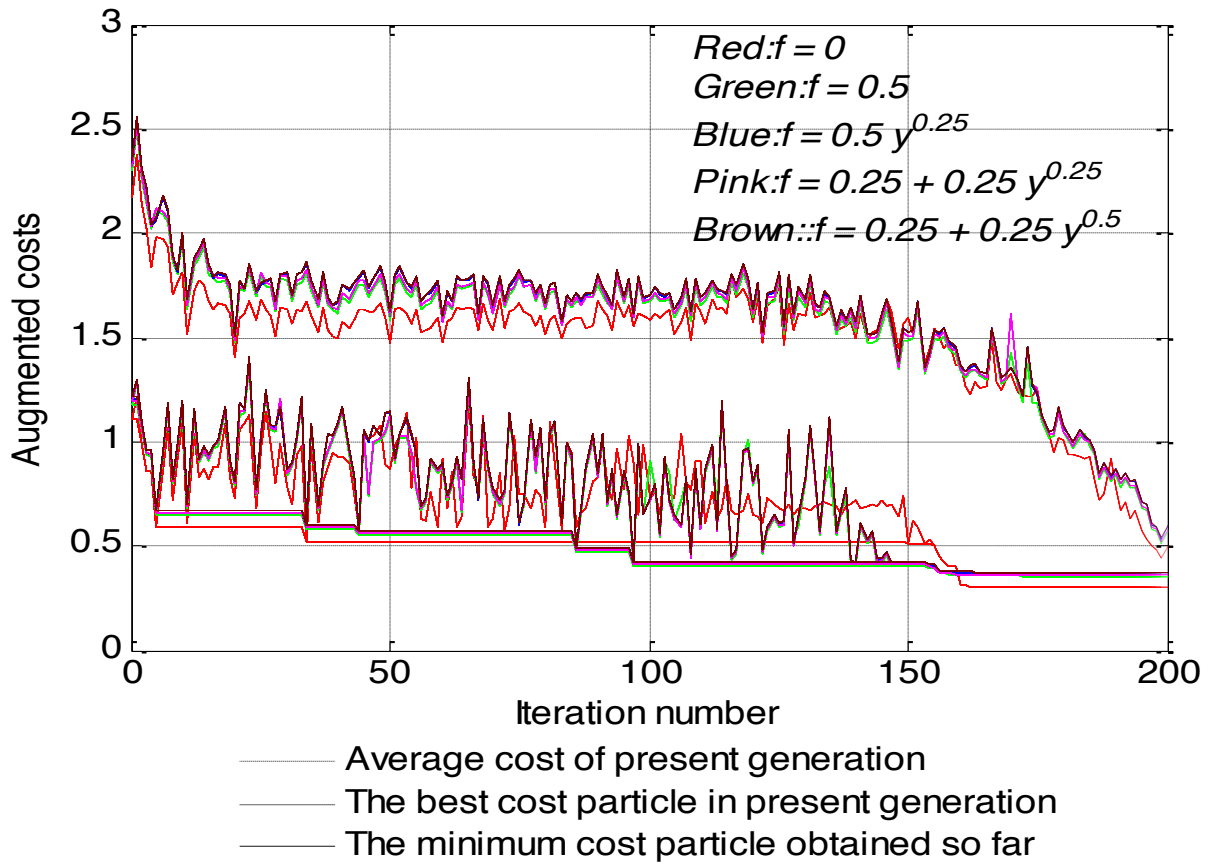


Figure 5.3a. The convergence trend of mean, local, and global dimensionless costs with iteration number for angular riprap stone for clear water flow condition near channel bottom

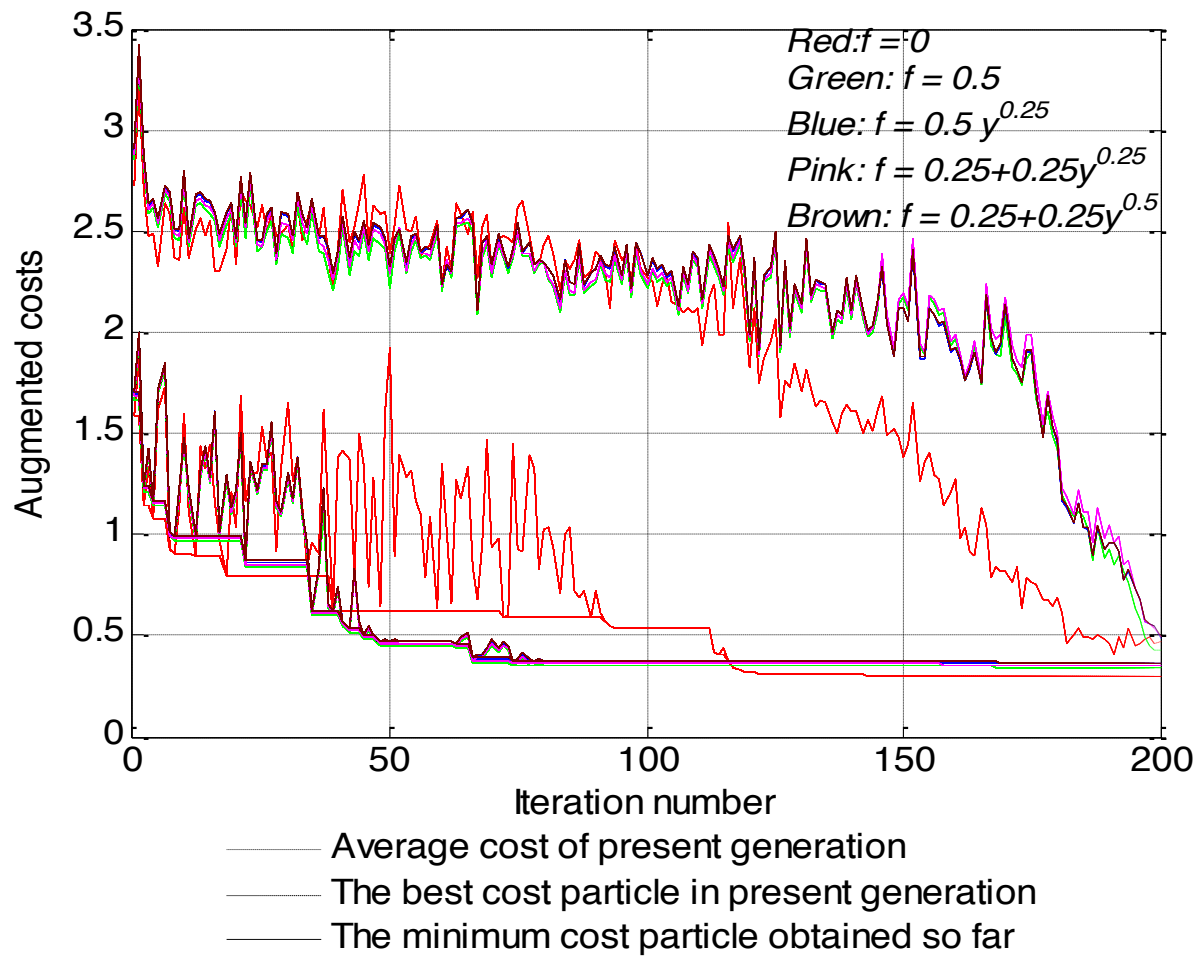


Figure 5.3b. The convergence trend of mean, local, and global dimensionless costs with iteration number for angular riprap stone for sediment laden flow condition near channel bottom

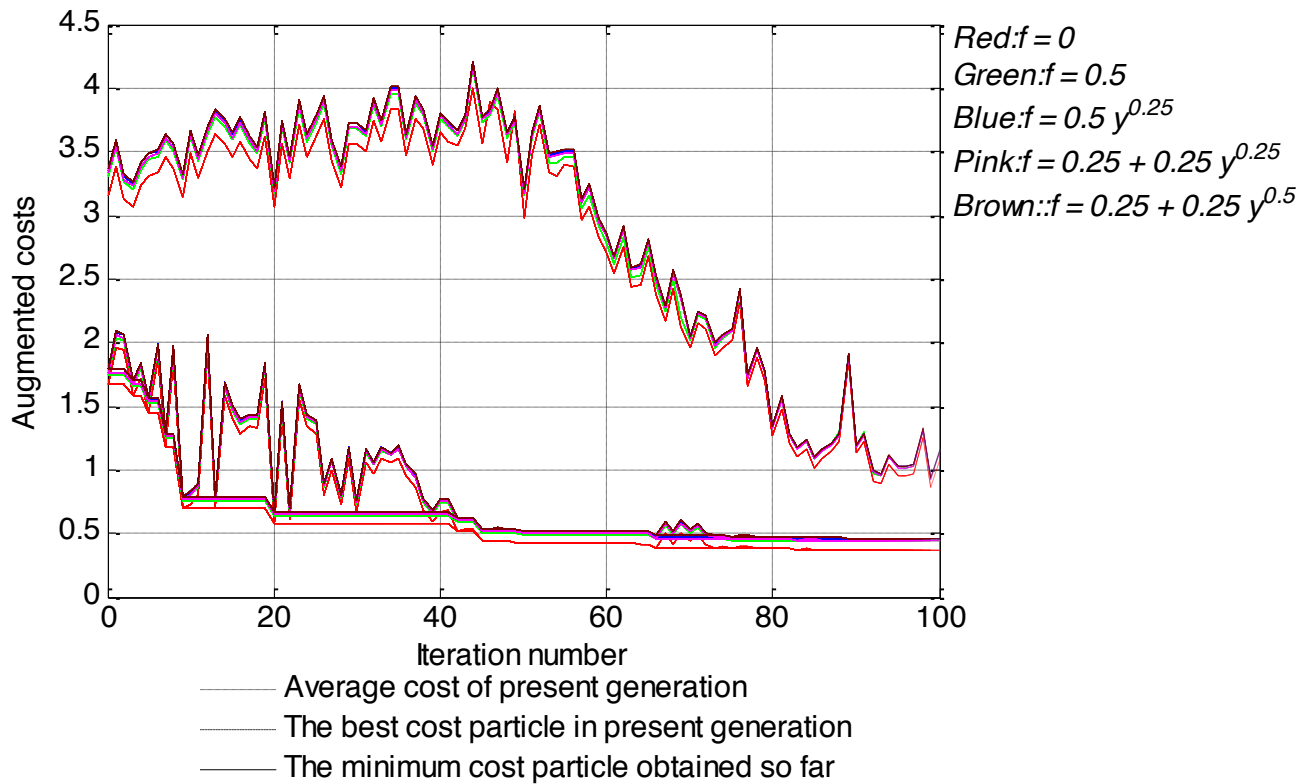


Figure 5.4a. The convergence trend of mean, local, and global dimensionless costs with iteration number for subround and subangular riprap stone for clear water flow condition near channel bottom

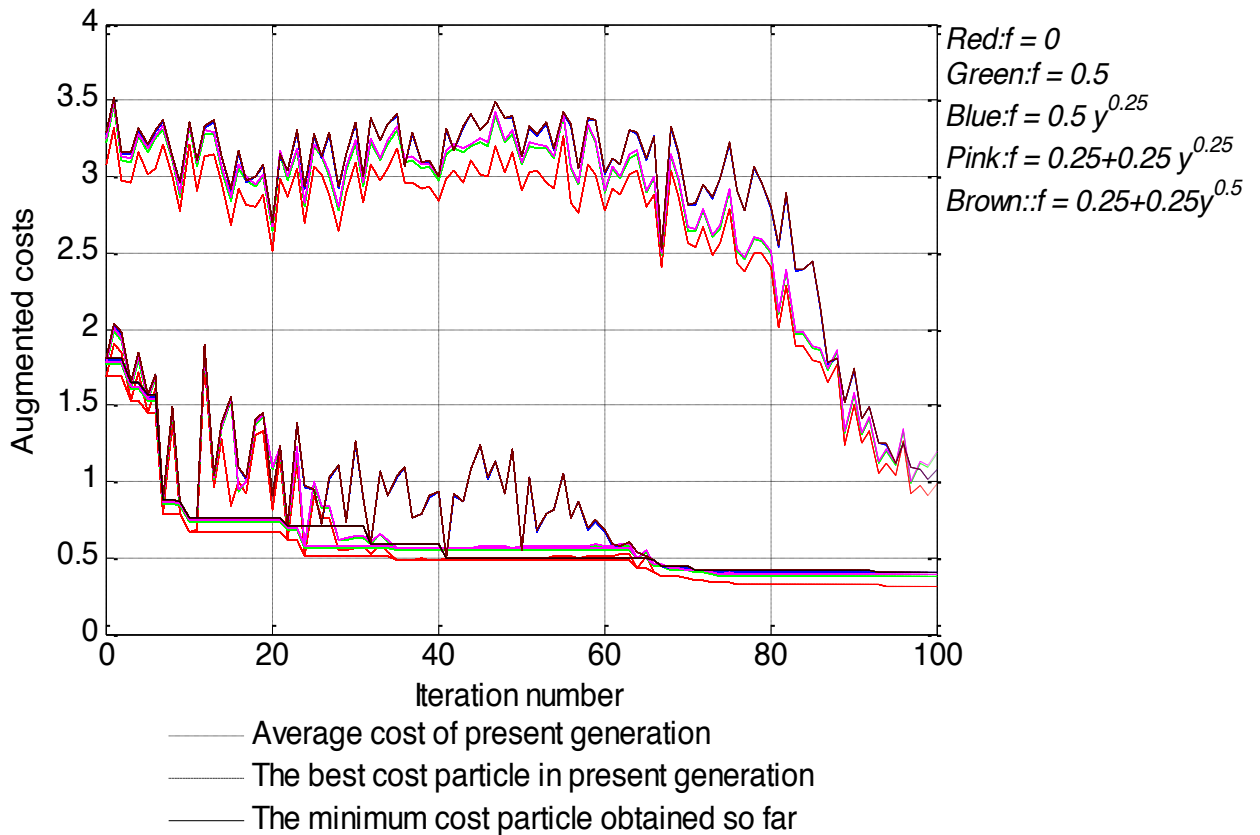


Figure 5.4b. The convergence trend of mean, local, and global dimensionless costs with iteration number for subround and subangular riprap stone for sediment laden flow condition near channel bottom

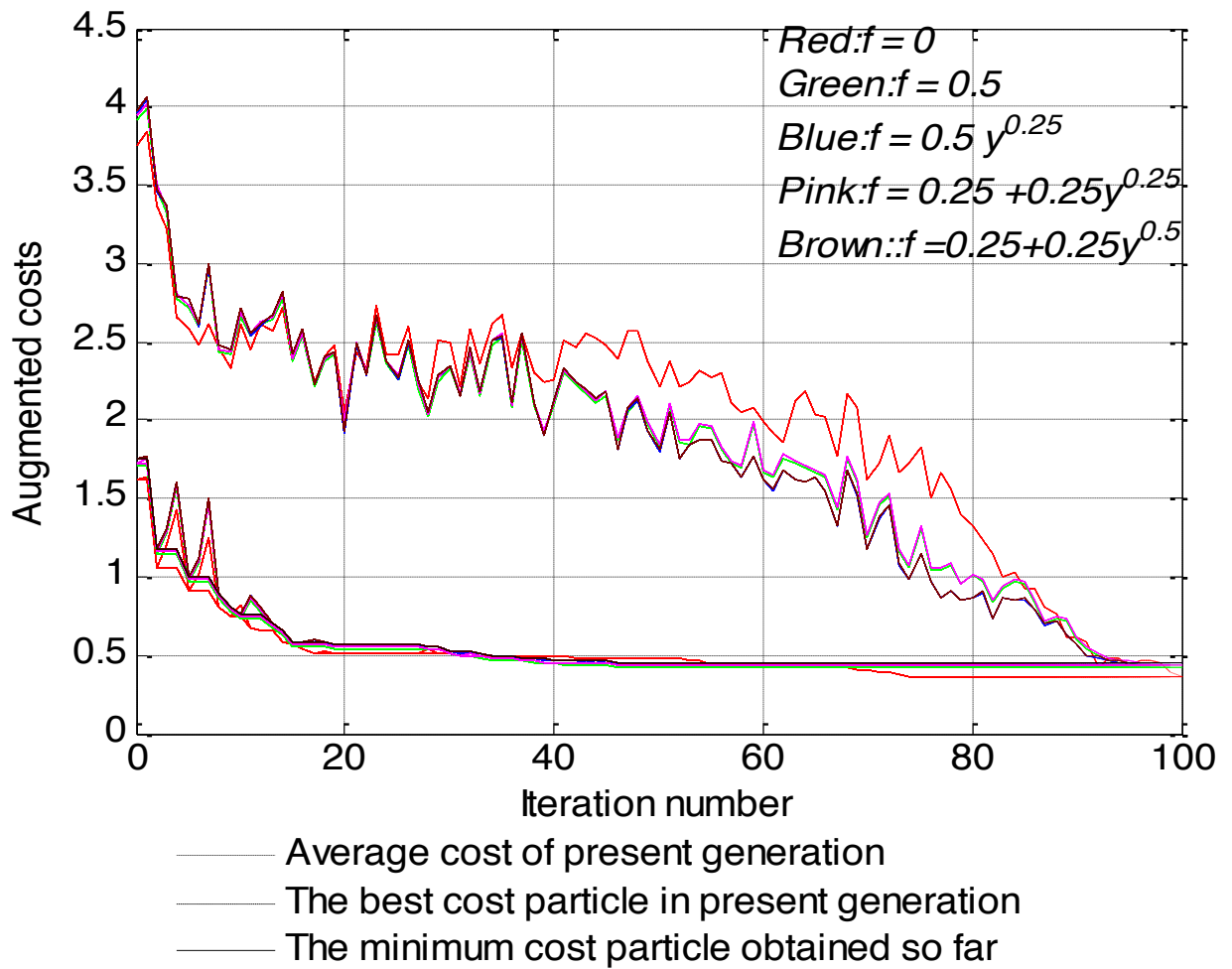


Figure 5.5a. The convergence trend of mean, local, and global dimensionless costs with iteration number for round riprap stone for clear water flow condition near channel bottom

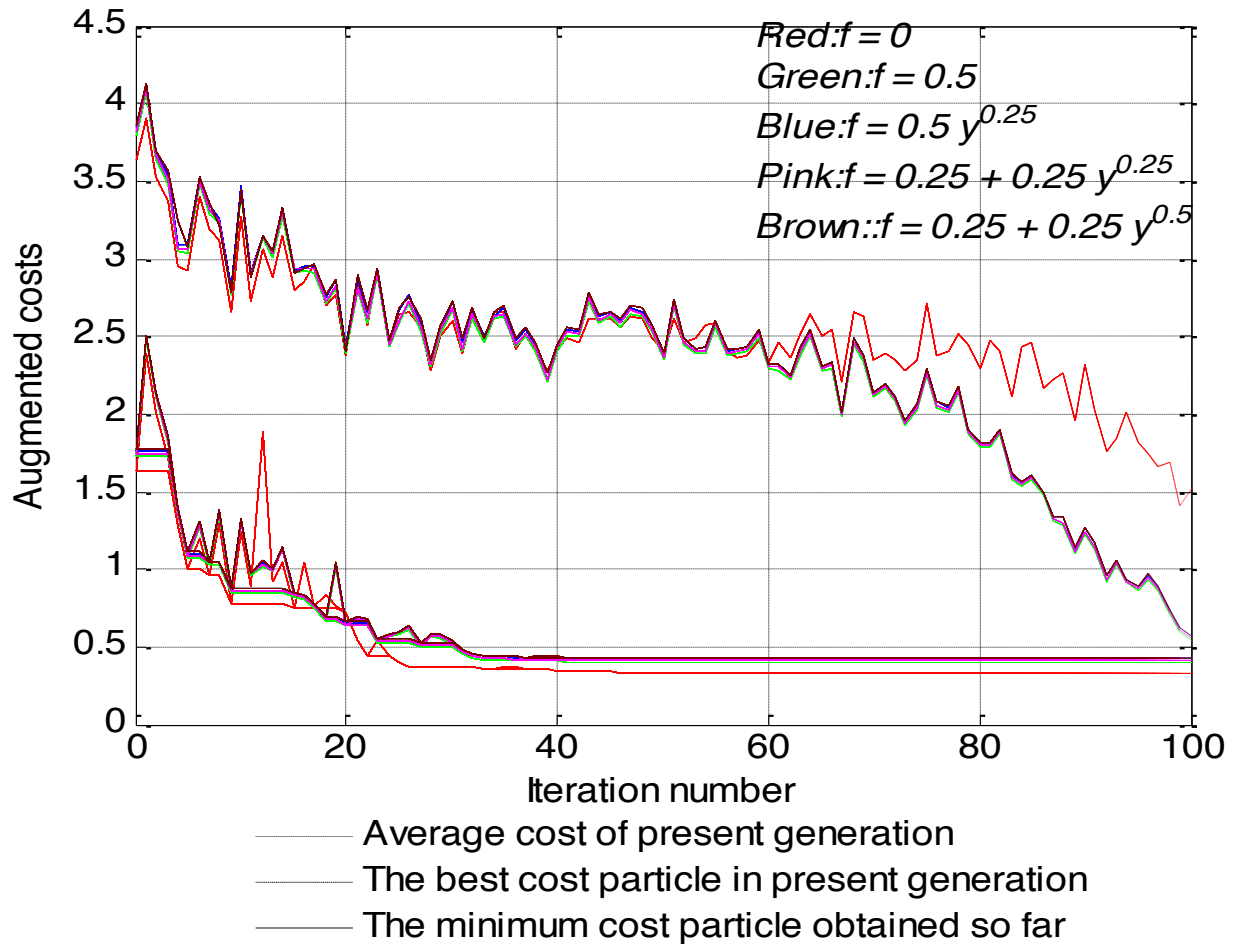


Figure 5.5b. The convergence trend of mean, local, and global dimensionless costs with iteration number for round riprap stone for sediment laden flow condition near channel bottom